

General Disclaimer

One or more of the Following Statements may affect this Document

- This document has been reproduced from the best copy furnished by the organizational source. It is being released in the interest of making available as much information as possible.
- This document may contain data, which exceeds the sheet parameters. It was furnished in this condition by the organizational source and is the best copy available.
- This document may contain tone-on-tone or color graphs, charts and/or pictures, which have been reproduced in black and white.
- This document is paginated as submitted by the original source.
- Portions of this document are not fully legible due to the historical nature of some of the material. However, it is the best reproduction available from the original submission.

**NASA TECHNICAL
MEMORANDUM**

NASA TM X-73650

NASA TM X-73650

**(NASA-TM-X-73650) FRICTION AND WEAR OF
SINTERED FIBER-METAL ABRADABLE SEAL
MATERIALS (NASA) 27 p HC A03/MF A01**

N77-23489

CSCL 11A

G3/37

**Unclassified
26166**

**FRICITION AND WEAR OF SINTERED FIBER-
METAL ABRADABLE SEAL MATERIALS**

by Robert C. Bill and Lawrence T. Shiembob
Lewis Research Center and
U. S. Army Air Mobility R&D Laboratory
Cleveland, Ohio 44135

**TECHNICAL PAPER to be presented at the
1977 International Conference on Wear of Materials
sponsored by the American Society of Mechanical Engineers
St. Louis, Missouri, April 25-28, 1977**



FRIC TION AND WEAR OF SINTERED FIBERMETAL
ABRADABLE SEAL MATERIALS

by Robert C. Bill

Lewis Research Center and
U.S. Army Air Mobility R&D Laboratory
and

Lawrence T. Shiembob
Pratt & Whitney Aircraft
East Hartford, Connecticut

ABSTRACT

Three abradable gas path seal material systems based on a sintered NiCrAlY fibermetal structure were evaluated under a range of wear conditions representative of those likely to be encountered in various knife-edge seal (labyrinth or shrouded turbine) applications. Conditions leading to undesirable wear of the rotating knife were identified and a model proposed based on thermal effects arising under different rub conditions. It was found, and predicted by the model, that low incursion (plunge) rates tended to promote smearing of the low density sintered material with consequent wear to the knife-edge. Trade-off benefits between base-line 19 percent dense material, a similar material of increased density, and a self-lubricating coating applied to the 19 percent dense material were identified based on relative rub tolerance and erosion resistance.

INTRODUCTION

The efficiency of gas turbine engines is becoming ever more important with the rise in energy costs and the concern over future fuel short-

ages. A critical consideration in achieving improved efficiency is the ability to maintain effective gas path sealing throughout the engine. In general, this means that operating clearances must be kept to a minimum, thus keeping efficiency losses due to leakage over blade tips and through labyrinth seals as low as possible. Typical gas path seal locations in a gas turbine engine are shown in Fig. 1 which shows typical compressor blade tip and knife edge seal locations.

One way to reduce leakage is to provide a stationary seal component that will preferentially wear, or abrade, during eccentric blade/seal interaction thereby minimizing the effect of the rub on blade/seal clearance. Figure 2 illustrates the benefit to be gained and shows that a 70 percent reduction in post rub clearance can be effected by providing an "abradable" or "rub tolerant" seal - one that is easily worn when a rub occurs.

Abradable seals are used in gas turbine engines today and the effort to develop improved system continues. There are three major requirements an abradable seal system must meet, the relative importance of each depending on the engine location. First, they must in fact be rub tolerant so that in the event of interaction with a blade tip or labyrinth knife edge, the vast majority of the wear occurs to the stationary seal material. Erosion resistance is also a requirement, since removal of the rub tolerant material by the high velocity gas and particulate in the stream would result in increased clearances. Finally, depending on the location in the engine, the rub tolerant seal material might have to survive in a severe thermal and corrosion environment.

The material properties needed to meet these requirements are often incompatible. For example, a high degree of rub tolerance is generally

associated with a low cohesive strength structure; on the other hand, erosion resistance demands that the material have a certain degree of cohesive strength. The nature of development of abradable seal systems is therefore concerned with the trade-off and optimizing of the abradability/erosion resistance relationship for a given engine operation.

The trade-off between erosion resistance and rub tolerance becomes more difficult for higher temperature application because generally higher strength systems are required to accommodate the higher temperature environment. As a result more abradable seal systems have been developed for the cooler engine locations such as the fan and low pressure compressor and conversely there exists a definite need for higher temperature abradable seal systems.

Low density (19 - 21 percent) sintered Hastelloy X fibermetal systems have demonstrated good performance and durability in compressor application. The purpose of this paper is to explore three variations of the fibermetal system that incorporate structural and compositional changes intended to provide increased temperature capability for turbine applications. Friction and wear characteristics were evaluated, and a model is purposed that accounts for the observed effects of various rub parameters. Erosion rates were also studied, showing the degree of trade-off possible between rub tolerance and erosion resistance.

APPARATUS AND PROCEDURE

Tests to evaluate rub tolerance and abradability of candidate gas path seal systems were performed in the dynamic abradability rig shown in Fig. 3. This rig consists of a rotor drive system and a seal specimen feed system.

The rotor drive system consists of an air turbine capable of driving disks up to 0.203 m (8.0 in.) diameter at speeds up to 40 000 rpm. Inter-changeable disks for either knife edge or blade tip configurations are bolted to one end of a horizontal spindle shaft. A knife edge configuration simulating low pressure turbine blade tip geometry was used for this program. The knife-edge was 5.08×10^{-4} M (0.020 in.) thick, and 2.54×10^{-3} M (0.100 in.) in height.

The seal specimen feed system consists of a dead-weight loaded carriage assembly to which the seal specimen is fastened by a suitable fixture. This carriage assembly can feed the specimen radially into the rotor at controlled rates from 2.54×10^{-6} m/s (0.0001 in./sec) to 5.08×10^{-4} m/s (0.020 in./sec). The radial motion of the specimen with respect to the rotor is defined as the incursion rate. Normal reaction force between the rotor and seal specimen is measured by a load cell installed in the carriage feed control system. For elevated temperatures tests, two oxy-acetylene heaters and an electric air heater were used as shown in Fig. 3. One of the oxy-acetylene heaters and the electric air heater were directed at the seal specimen surface. The other oxy-acetylene heater was directed at the back of the seal specimen. The oxy-acetylene heater directed at the seal surface was turned off immediately before the rub interaction to prevent knife edge heat damage. The second oxy-acetylene heater and electric air heater were effective in maintaining seal specimen temperature after the front heater was extinguished.

Rotor speed, seal specimen temperature at the center of the rub area, carriage travel, normal load and torque are recorded continuously during rub interaction. Speed is sensed by a magnetic pulse

counting system built into the drive turbine. Seal specimen temperature is measured with an optical pyrometer system. A linear voltage transformer system is used to measure carriage assembly travel. Knife edge torque is measured with a Vibrac torque meter which uses a calibrated shaft, two slotted disks and a light beam sensor which measures the twist in the calibrated shaft by the amount of light transmitted through the window opened by relative rotation of the slotted disks. These parameters were all recorded simultaneously on a multi-channel high-speed lightbeam stripchart.

Seal and rotor wear were measured after test and a volume wear ratio or volume pick-up ratio was calculated as a basis for relative rub tolerance comparison. The volume ratio was defined as the amount of rotor wear or pickup divided by the seal wear volume. Small values for the volume wear ratio are desirable; ideally zero.

The erosion equipment used in the program was designed to test abradable materials for turbine tip sealing under simulated engine conditions. The rig consists of a combustor, a temperature equalizing (mixing) chamber, a specimen chamber and provisions for introducing erosive particles into the gas stream at a controlled rate. Particulate erosion testing described in this report was conducted with size 80 grit, Al_2O_3 particles injected into the gas stream with a particulate mass flow rate of approximately 6 lb/hr. Testing was conducted with a gas velocity of 0.35 Mach number and impingement angle of 7 degrees.

Seal Systems Evaluated

A 19 percent dense NiCrAlY fibermetal served as a baseline. The system is similar to the 19 percent Hastelloy X fibermetal currently used in compressor air seals except that the material was changed for

higher temperature capability. The fibermetal structure consists of metal fibers having an aspect ratio of about 5 or 6 to 1, and a nominal fiber diameter of 8 micrometers. A combination of mechanical densification and sintering results in the desired final density, in this case 19 percent. The NiCrAlY alloy composition is Cr 15 percent, Al 9.5 percent, Y 0.2 percent, and the balance nickel.

In an attempt to improve the erosion resistance and oxidation life of the fibermetal system, a fibermetal system of 33 percent density with larger particle size was fabricated. Particles of 25 micrometer diameter with an aspect ratio of 5 or 6 to 1 were employed in the 33 percent dense structure. The same NiCrAlY alloy was used as in the 19 percent dense formulation.

Another approach to providing a material with improved erosion resistance combined with rub tolerance was to plasma spray a nichrome-glass composite onto a 19 percent dense NiCrAlY feltmetal substrate. The sprayed nichrome glass (ref. 1), has demonstrated good friction and wear properties when used as a self-lubricating coating for high temperature sliding applications.

The glass constituent was intended to serve two purposes: first to enhance the oxidation resistance of the NiCr through formation of a continuous coating on NiCr particles; second, to provide a self-lubricating capability for the coating. Through thermal softening the glass can provide an easily shearable layer on the rub surface, thereby promoting rub tolerance.

The exact composition of the coating was 80 percent nichrome (nickel-20 percent chromium) and 20 percent glass (consisting of 58 percent SiO_2 , 21 percent BaO , 8 percent CaO , and 13 percent K_2O). As sprayed, the

coating was about 500 micrometers (0.020 in.) thick. It was intended that the interaction loads would be maintained at a low level by virtue of the low density, compliant feltmetal substrate. It was also intended that the low density substrate would accommodate thermal mismatches between the seal coating and the engine component on which it might be mounted.

RESULTS

Figure 4 shows the friction torque results of the room temperature tests as a function of incursion rate.

The friction of the 19 percent dense fibermetal was the lowest of the materials studied, and was rather insensitive to incursion rate (radial motion of the specimen with respect to the rotor) at a 305 m/sec rotating speed (Fig. 4(a)). At 183 m/sec (Fig. 4(b)), increased friction was observed at the highest incursion rate. Comparison of Figs. 4(a) and (b) shows that for the two lower incursion rates, the rotational speed did not significantly affect the frictional torque.

The 33 percent dense fibermetal showed a trend of increasing friction with incursion rate at 305 m/sec (Fig. 4(a)).

The coated fibermetal showed a slight tendency toward reduced friction with increased incursion rate for both rub speeds. Comparison of Figs. 4(a) and (b) shows that the friction was significantly higher at the lower rub speed. The friction for the coated fibermetal was higher than that for the uncoated materials.

The wear results summarized in Figs. 5(a) and (b) demonstrate two trends. First, minimum knife-edge wear was observed at the intermediate incursion rate for 19% dense fibermetal, a tendency most noticeable at the 183 m/sec rotating speed. Second, knife-edge wear was

observed to be maximum under low incursion rate conditions for 33% dense fibermetal and coated fibermetal.

In one case a test was conducted on 33% dense fibermetal under high incursion rate conditions using an exceptionally rough knife-edge. Very high knife edge wear was observed and attributed to the exceptional roughness. This position is supported by the following considerations. As shown in Fig. 6, tests conducted at 1366 K (2000° F) showed a general trend toward less wear and more pickup as incursion rate was increased. On a comparable basis this would indicate that at ambient temperature the 25.4×10^{-6} m/sec test would be expected to result in pickup. In addition, a repeat test at 25.4×10^{-6} m/sec as shown in Fig. 6 with a knife edge machined as "smooth" as possible resulted in reduced knife edge wear. The knife edge used in this repeat test, was machined to a maximum radial run-out of 5×10^{-6} m compared to a standard of $25-30 \times 10^{-6}$ m.

The effects of temperature on the friction and wear results are shown in Fig. 7 for a 305 m/sec rub speed and a 25.4×10^{-6} m/sec incursion rate. Temperature does not seem to have a systematic effect on friction as may be seen in Fig. 7(a). Wear results shown in Fig. 7(b) do suggest increased knife edge wear as temperature is increased.

Examination of the 19 and 33 percent dense fibermetal surfaces after undergoing rub interaction revealed varying degrees of glazing, or smearing of the fibermetal on the rub surface. In the case of light smearing or no smearing, individual particles of fibermetal could be identified in the rub groove surface. An example of such a rub surface, accompanied by a section view, is shown in Fig. 8. Medium smearing describes a situation in which the discrete fibermetal particles are partly obscured by a densified, plastically deformed rub surface; the

smeared rub surface, however, is only about 50 percent continuous. A heavily smeared rub surface is one on which the discrete fibermetal particles are totally obscured by a plastically deformed layer completely covering the rub groove surface. An example of a heavily smeared rub groove is shown in Fig. 9.

The room temperature tests in which the rub speed was 183 m/sec all resulted in a lightly smeared or nonsmeared surface. The following generalizations regarding smearing for the 305 m/sec room temperature tests were made: (1) Light smearing or no smearing was observed for all cases in which transfer of seal material to the knife edge occurred; (2) Light smearing or no smearing was seen on 19 percent dense fibermetal rub surfaces; (3) Heavy smearing was seen on the 33 percent dense fibermetal rib surfaces after tests that resulted in knife edge wear; and (4) Reduced incursion rate resulted in increased smearing tendency.

Elevated temperature tests run at 305 m/sec with a 25.4×10^{-6} m/sec incursion rate showed light smearing or no smearing for the 19 percent dense fibermetal and the coated fibermetal. Medium smearing was observed for the 33 percent dense fibermetal at 1050 and 1120 K.

The results of the erosion evaluation are shown in Fig. 10. Steady state erosion rate (calculated from weight loss measurements) is shown as a function of temperature for the three seal materials investigated. The most erosion resistant material is the nichrome-glass coated fibermetal showing an erosion rate less than 1/10 that of uncoated 19 percent dense fibermetal at low temperature. The erosion rate of 33 percent dense fibermetal was 1/6 to 1/4 that of 19 percent dense fibermetal over the temperature range. The erosion rate of the nichrome-glass coating was not seen to increase with temperature, unlike the uncoated fibermetal.

DISCUSSION

Qualitatively, the friction trends obervations for the experimental gas path seal materials are consistent with trends reported in the literature. The effect of rotor speed on the friction of 33 percent dense fibermetal and coated fibermetal correlates with temperature effects seen for nickel base materials. A reduction in friction is reported at temperatures above 1400⁰ F for nickel based alloys (Refs. 2 and 3), corresponding to changes in oxidation kinetics under sliding conditions. Thus, the higher rotor speeds which would result in higher temperatures at the knife-edge/seal interface, can be expected to lead to reduced friction.

Quantitatively, however, the friction coefficient values do not agree so well with published results. The maximum friction coefficient observed for the coated fibermetal was 0.2, with friction coefficients of 0.1 and less for the 19 and 33 percent dense fibermetal. These values are much less than expected for sliding metal surfaces (Refs. 2 to 4). Most likely this is because fracture of discrete particles from the seal material occurs simultaneously with the surface frictional mechanisms, effectively reducing the maximum shear force that can be supported by the rub surface.

The key factor influencing the wear behavior of 19 and 33 percent dense NiCrAlY fibermetal is the occurrence of smearing, or glazing. A General trend of increased glazing, with consequent increased wear to the knife-edge, was seen to occur for decreasing incursion rates. This trend can be explained in terms of thermal effects associated with the incursion rate.

Consider the frictional heat generation at the sliding interface, and

consequent heat fluxes into the rotating knife-edge and abradable body. The following equation which is essentially the equation for steady state ablation with the coordinate system tied to the moving interface, approximates the thermal response of the abradable body:

$$\frac{\partial}{\partial(x)} \left(K_{AM} \frac{\partial T}{\partial x} \right) = -\dot{\Delta} \rho C \frac{\partial T}{\partial x} \quad (\text{see Ref. 5}) \quad (1)$$

$$T = T_{cr} \text{ at } x = 0$$

$$T = T_{\infty} \text{ at } x = \infty \text{ (bulk temperature)}$$

where ρ , C , and K_{AM} are the density, specific heat, and thermal conductivity of the abradable, or rub tolerant material. The term $\dot{\Delta}$ is the linear rate of rub tolerant material loss at the rub surface. For highly rub tolerant materials, with low volume wear factors, $\dot{\Delta}$ is nearly equal to the incursion rate. T_{cr} is an assumed limiting temperature that may be approached at the rub interface. This limiting temperature might be identified as a dynamic softening temperature (Ref. 6), or the point of incipient melting at the rub interface as suggested in reference 7.

Implicit in Eq. (1) is the assumption that steady state conditions are reached in the moving coordinate system, advancing at a rate of $\dot{\Delta}$, as shown in Fig. 11. For large values of x (compared to the 0.020 in. contact width), Eq. (1) becomes a less accurate approximation as three dimensional heat flux effects become important. As a further qualification it should also be recognized that the seal material does not really approach being a semi-infinite body, so the second boundary condition represents another approximation. Nevertheless, Eq. (1) will be developed to illustrate qualitative effects that help explain the observed wear phenomena.

The solution to Eq. (1) may be expressed as:

$$\frac{T - T_{\infty}}{T_{CR} - T_{\infty}} = \exp\left(\frac{-\dot{\Delta}x}{\alpha}\right) \quad \alpha = \frac{K}{\rho c} \quad (2)$$

thus giving the temperature distribution in the abradable material. Note the inverse exponential dependency on $\dot{\Delta}$. The total heat generation and associated heat balance expression for the sliding interface is given by:

$$\begin{aligned} \dot{Q} &= \mu PV \\ &= K_{KE} \left(\frac{\partial T}{\partial x} \right)_{x=0^-} - K_{AM} \left(\frac{\partial T}{\partial x} \right)_{x=0^+} + \rho \Delta C (T_{CR} - T_{\infty}) \end{aligned} \quad (3)$$

where

μ coefficient of friction

P contact pressure

V sliding velocity

From Eq. (2),

$$\left(\frac{\partial T}{\partial x} \right)_{x=0^+} = -(T_{CR} - T_{\infty}) \frac{\dot{\Delta}}{\alpha}$$

So

$$\dot{Q} = PV - K_{KE} \left(\frac{\partial T}{\partial x} \right)_{x=0^-} + K_{AM} (T_{CR} - T_{\infty}) \frac{\dot{\Delta}}{\alpha} + \rho \Delta C (T_{CR} - T_{\infty})$$

An expression for the steady state heat flux into the rotating knife edge

$K_{KE} \left(\frac{\partial T}{\partial x} \right)_{x=0^-}$ now follows:

$$\begin{aligned} K_{KE} \left(\frac{\partial T}{\partial x} \right)_{x=0^-} &= \mu PV - K_{AM} (T_{CR} - T_{\infty}) \frac{\dot{\Delta}}{\alpha} \\ &\quad - \rho_{AM} \Delta C_{AM} (T_{CR} - T_{\infty}) \end{aligned} \quad (4)$$

Two important conclusions may be drawn from Eqs. (2) and (4): First, the temperature at a given depth below the rub surface decreases exponentially with Δ , resulting in temperature profiles like those shown in Fig. 11; second, provided μ and P are not affected by the rub action, heat flux into the knife edge decreases with increasing Δ . The significance of the first conclusion is that low incursion rates would promote softening of the seal material particles below the rub surface, increasing the smearing tendency and promoting greater heat generation and wear to the knife edge. The second conclusion is consistent with the observed trend of increased knife edge wear under low incursion rate conditions, as increased heat flux into the knife-edge would lead to softening of the knife-edge material.

Recall that the results shown in Fig. 11 depict steady state conditions in the moving coordinate system. Order of magnitude calculations using

$$T - T_{\infty} = \frac{2Q_{AM}}{K_{AM}} \left(\frac{\alpha T}{\pi} \right)^{1/2} e^{-x^2/4\alpha t} - \frac{x}{2} \operatorname{erfc} \frac{x}{2\alpha t} \quad (\text{Ref. 10})$$

suggest that at a depth of $2.54 \cdot 10^{-5}$ m (0.01 in.) below the rub surface a temperature of about 600° F is reached in one second. It was assumed that half of the frictional heat generated flowed into the abradable material; $\mu \approx 0.1$; $P \approx 2$ lb per inch of contact length; sliding speed was 305 m/sec (1000 ft/sec); $K_{am} \approx 0.1$ Btu/hr ft $^{\circ}$ F (low density sintered material); and $\alpha \approx 10^{-5}$ ft 2 /sec. Thus, the temperature profiles shown in Fig. 11 would be closely approached at the low and intermediate incursion rates; at the high incursion rate, the temperature gradient in the abradable material would be even steeper than indicated.

In addition to the thermal effects, there is also a geometric effect. Under low incursion rate conditions, only the tips of a few high spots on the knife edge participate during a rub. The frictional heat generated during the removal of discrete particles of seal material encountered during a given incursion distance is then split between the seal material and a very small fraction of the rotating knife-edge circumference. Such a heat split situation can result in thermoelastic growth of the contact points (Ref. 8).

The nichrome-glass sprayed layer applied to the low density fiber-metal substrate was intended to enhance the erosion resistance of the fibermetal seal material. Under rub conditions, the normal load was accommodated by a densified fibermetal substrate beneath the glazed coating rub surface, as may be seen in Fig. 12. The normal loads were similar to those measured in the case of the glazed 33 percent fibermetal rub tests. This effect, in conjunction with self-lubricating capabilities of the glass constituent (Ref. 1) promoted low knife-edge wear under some rub conditions. The rub performance of the coated fibermetal can probably be further improved through attempts to optimize the coating thickness and composition.

In comparison to sintered materials of a density approaching that of the sprayed coating, the coated fibermetal system provided for superior rub tolerance at the higher incursion rate (Ref. 9) due probably to the combination of compliant substrate and self-lubricating coating properties.

Essentially, the sprayed layer represented a trade-off between greatly enhanced erosion resistance (Fig. 10) at the cost of reduced rub tolerance. This kind of trade-off is typical of the dilemma in gas

path sealing, brought on by conflicting material requirement for rub tolerance and erosion resistance. The 33 percent fibermetal provides another example of this tradeoff. Greatly improved erosion resistance over the 19 percent dense material was gained at the cost of a slight sacrifice in rub tolerance. Obviously for a given application an optimum material formulation representing a balance between acceptable rub tolerance and a necessary degree of erosion resistance exists. The three materials presented and discussed in this paper illustrate the range of balance achievable between these requirements using a single basic approach - that of applying a low density material and modifying its structure and configuration.

A further aspect of the coated low density metal approach, again requiring optimization, is the possibility of the low density substrate affording a compliant buffer between the engine casing and the seal surface. One of the functions of such a buffer would be to absorb thermal expansion mismatch due to property and temperature gradients between the seal surface and the casing.

CONCLUSIONS

The study of high speed sliding wear of potential abradable seal materials as might be encountered in labyrinth gaspath seal applications, indicates the following:

1. The development of a continuous, plastically smeared rub surface on the abradable material leads to accelerated knife-edge wear.
2. The tendency to promote smearing is increased when the incursion rate is low, most likely due to thermal effects.
3. Application of a dense, self-lubricating coating to a fibermetal substrate provided a promising combination of rub tolerance and erosion resistance.

4. A thermal model, based on one-dimensional heat conduction effects, was in qualitative agreement with the observed experimental results.

REFERENCES

1. Sliney, H. E., "Self-Lubricating Plasma-Sprayed Composites for Sliding Contact Bearings to 900° C," NASA TN D-7556, Feb. 1974.
2. Foley, R. T., Peterson, M. B., and Zapf, C., "Frictional Characteristics of Cobalt, Nickel and Iron as Influenced by Their Surface Oxide Films," ASLE Transactions, Vol. 6, 1963, p. 29.
3. Rabinowicz, E., "Lubrication of Metal Surfaces by Oxide Films," ASLE Transactions, Vol. 10, 1967, p. 400.
4. Kragelski, I. V., Friction and Wear. Butterworths, Wash., 1965, p. 158.
5. Rohsenow, W. M. and Choi, H. Y., Heat Mass and Momentum Transfer, Prentice Hall, Inc., Englewood Cliffs, N. J., 1961, p. 122.
6. Bill, R. C. and Wisander, D. W., "Recrystallization as a Controlling Process in the Wear of Some F.C.C. Metals." Wear, Vol. 41, 1977, p. 351.
7. Ho, Ting-Long, "Some Wear Studies on Aircraft Brake Systems," Rensselaer Polytechnic Institute, Troy, N. Y., Oct. 1975; also NASA CR-134989.
8. Kilaparti, S. R. and Burton, R. A., "Pressure Distribution for Patch-like Contact in Seals with Frictional Heating, Thermal Expansion and Wear," Journal of Lubrication Technology, Vol. 98, 1976, p. 596.
9. Shiembob, L. T., "Development of Abradable Gas Path Seals," PWA-T-5081 Pratt and Whitney Aircraft, East Hartford, Conn., 1975; also NASA CR-134689.

10. Carslaw, H. S. and Jaeger, J. C., Conduction of Heat in Solids,
Oxford at The Clarendon Press, 1959, p. 75.

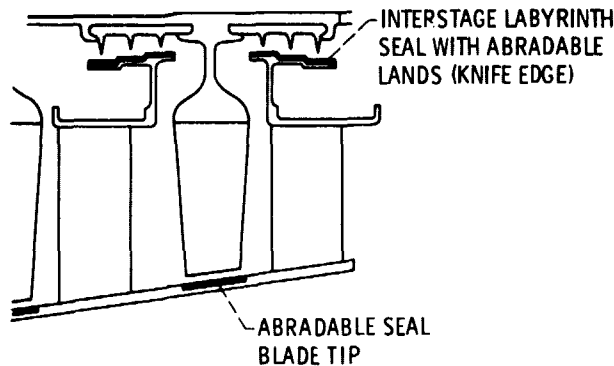


Figure 1. - Typical gas path seal locations.

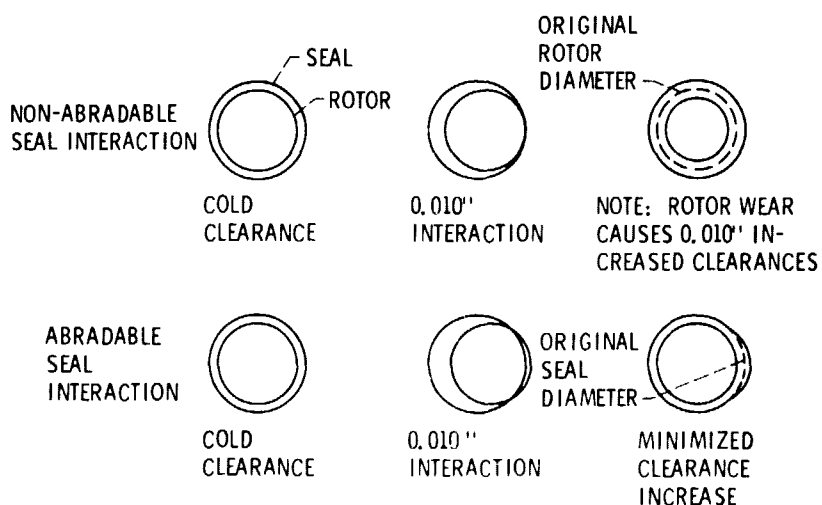


Figure 2. - Effects of rub interactions on gas path seal clearances.

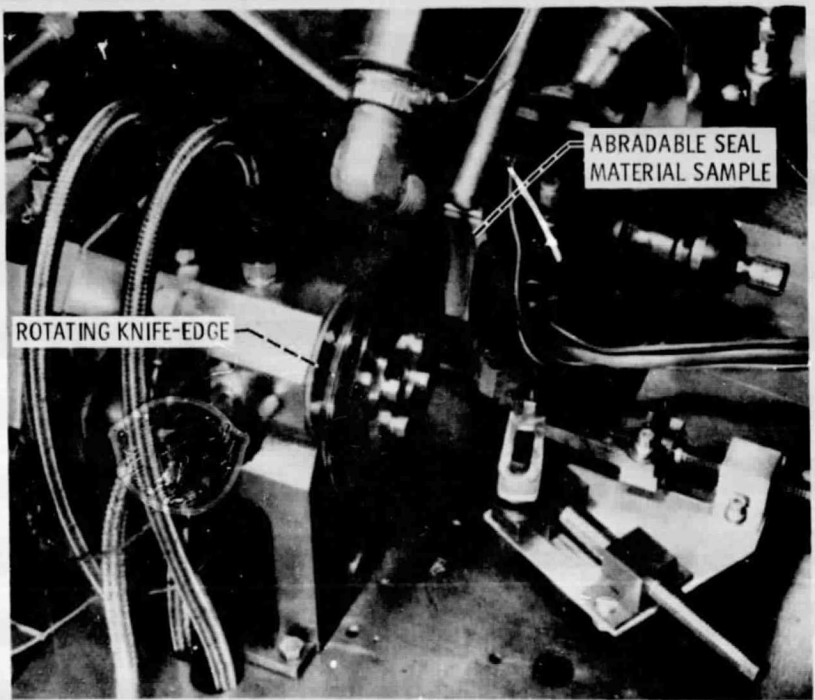


Figure 3. - Abradable seal test apparatus.

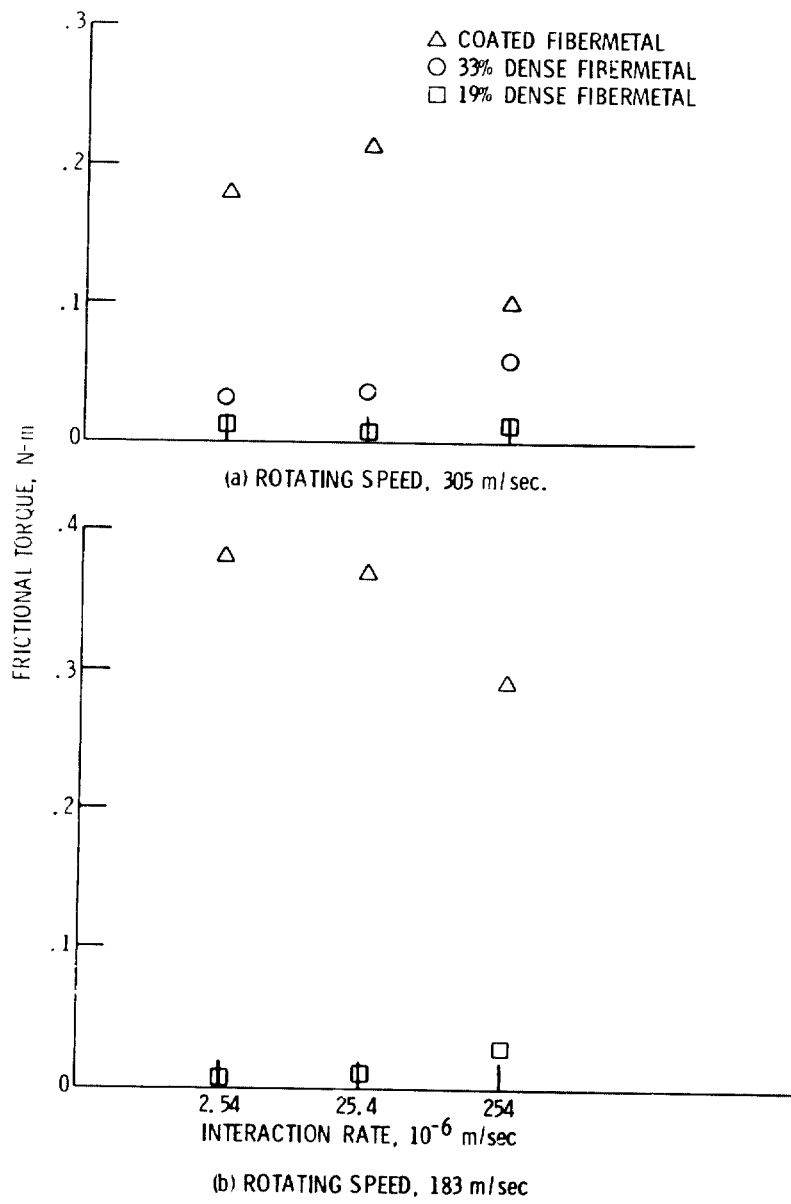


Figure 4. - Friction torque versus interaction rate for three gas path seal materials. Tests were conducted at room temperature.

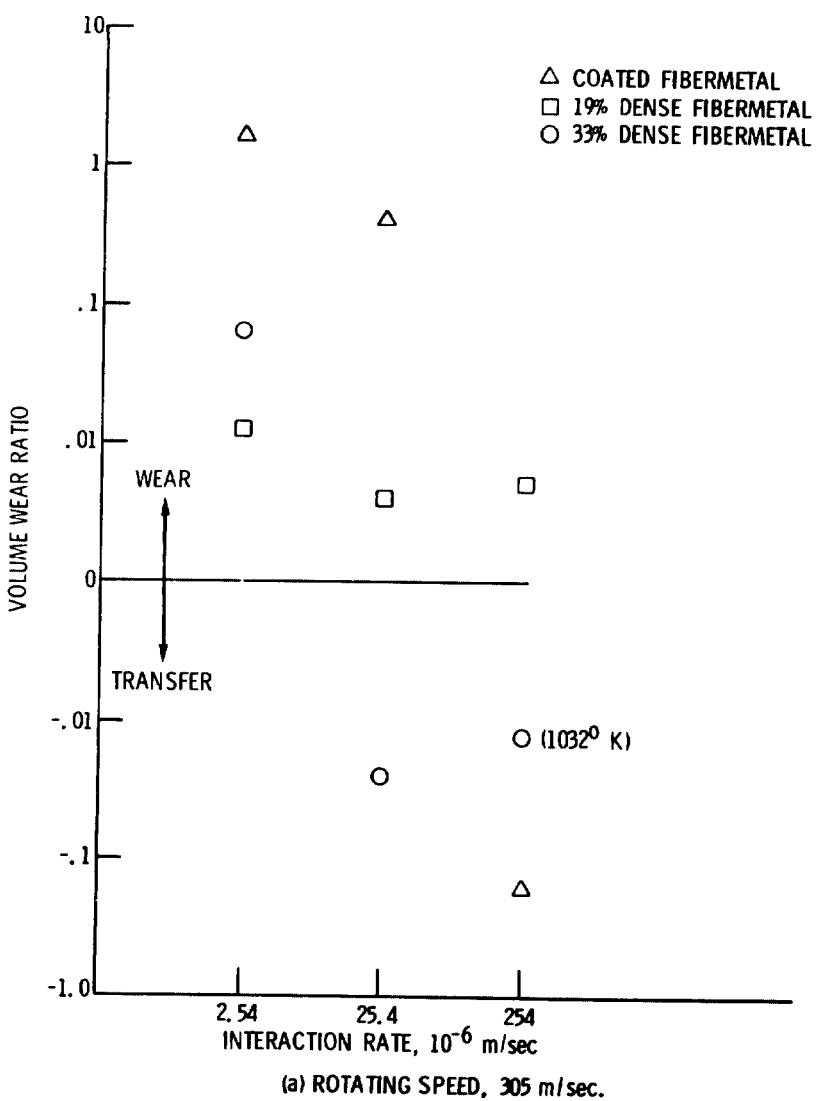
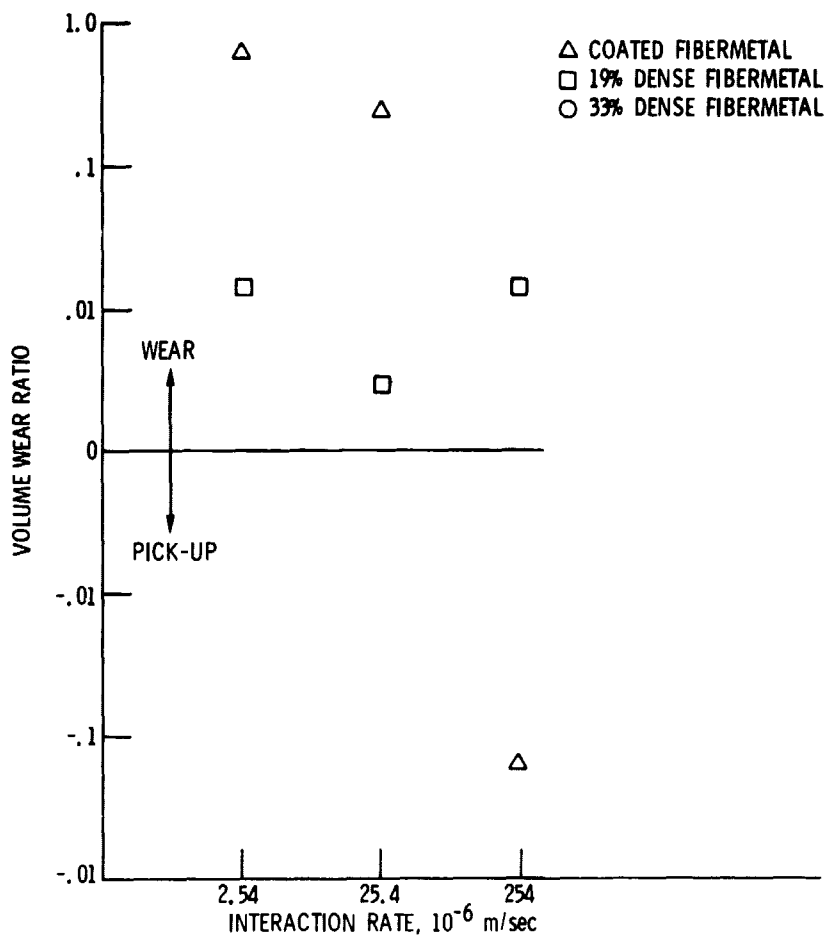


Figure 5. - Volume wear ratio versus interaction rate.



(b) ROTATING SPEED, 183 m/sec.

Figure 5. - Concluded.

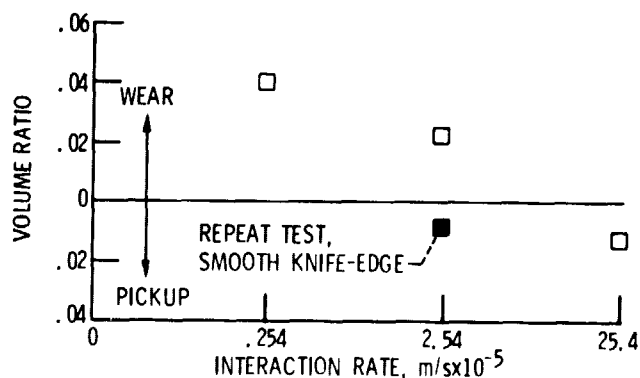


Figure 6. - Volume wear ratio versus incursion rate for 33 percent dense fibermetal. Surface speed was 305 m/sec and temperature was 1366° K.

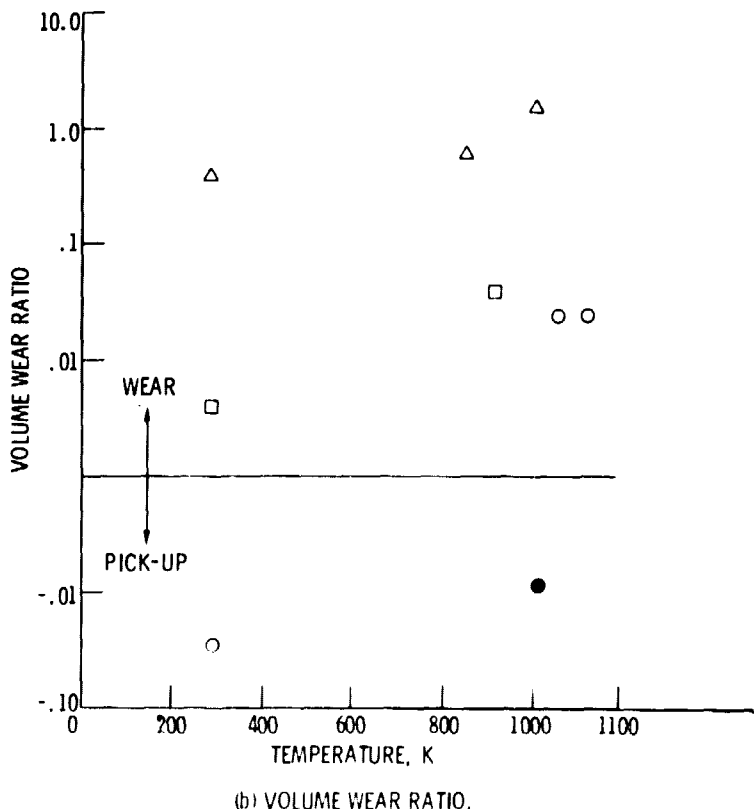
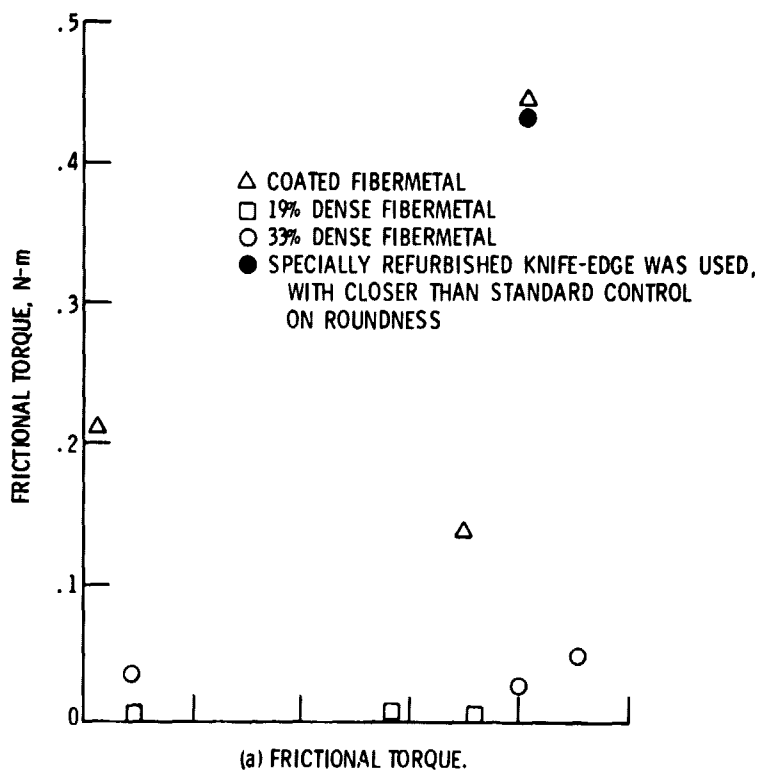


Figure 7. - Frictional torque and volume wear ratio as functions of temperature. Rotating speed, 305 m/sec; interaction rate, 25.4×10^{-6} m/sec.

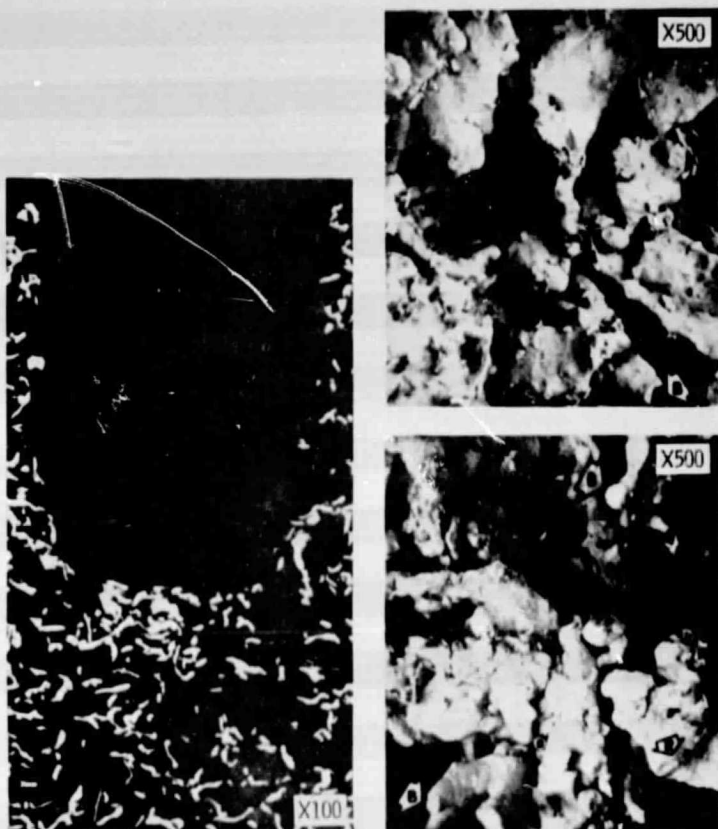


Figure 8. - 19 Percent dense NiCrAlY fibermetal after interaction with a knife-edge at 183 m/sec rotational speed, 25.4×10^{-6} m/sec incursion rate at room temperature. (a) Microsection of the rub groove; (b) and (c) SEM photographs of the rub surface. "B" indicates debond sites; "R" indicates a rub effect on a particle.

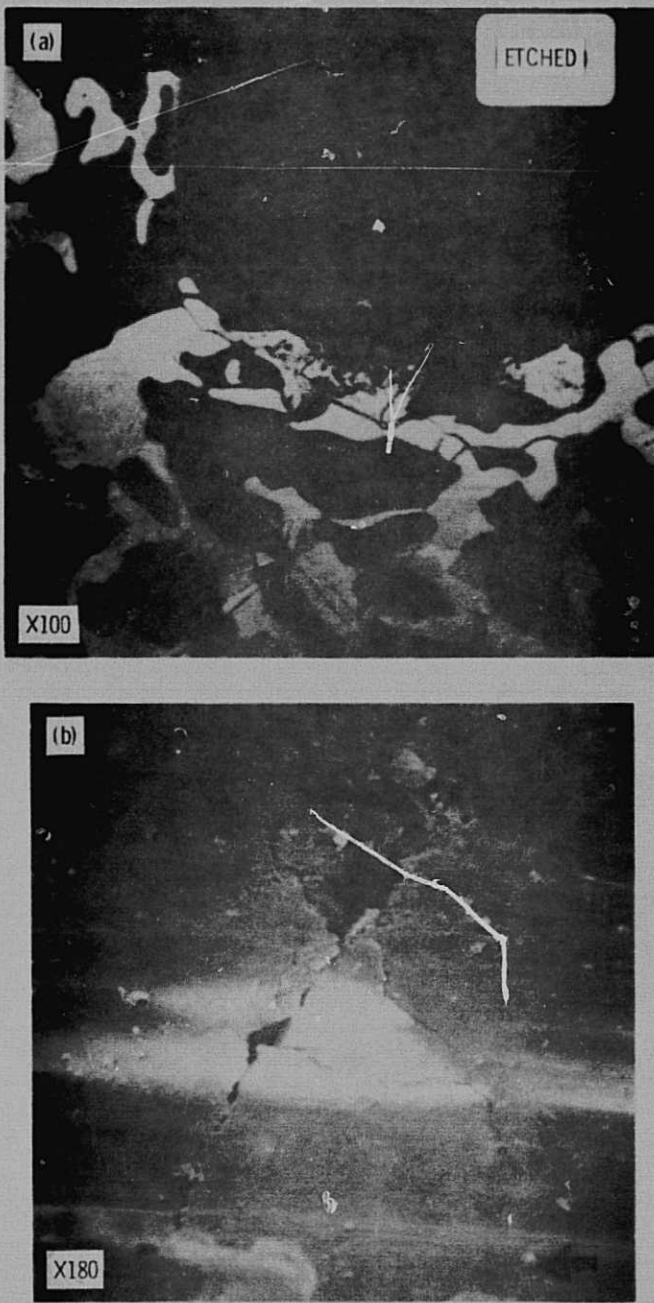


Figure 9. - 33 Percent dense NiCrAlY fibermetal after interaction with a knife-edge at 305 m/sec rotational speed, 25.4×10^{-6} m/sec incursion rate, 1116^0 K. (a) Microsection of the rub groove; (b) SEM photograph of the rub surface.

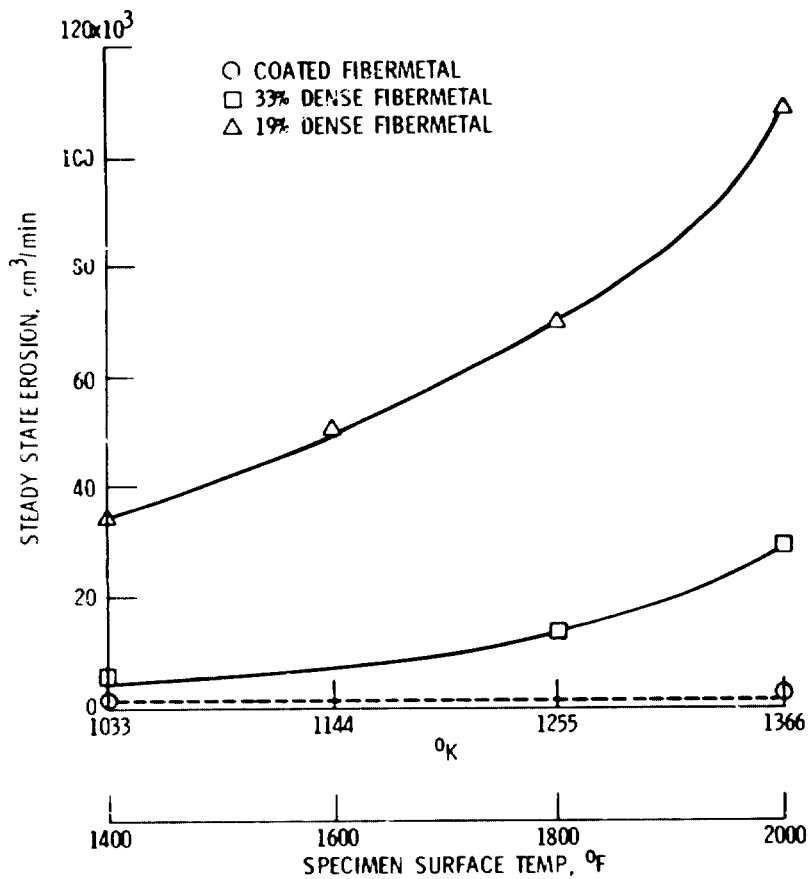


Figure 10. - Volume loss particulate erosion rates as function of temperature for turbine gas path seal candidate materials.

KNIFE-EDGE MATERIAL (ROTATING)		ABRADABLE MATERIAL	
K_{KE}	Thermal Conductivity	K_{AM}	Thermal Conductivity
ρ_{KE}	Density	ρ_{AM}	Density
C_{KE}	Specific Heat	C_{AM}	Specific Heat

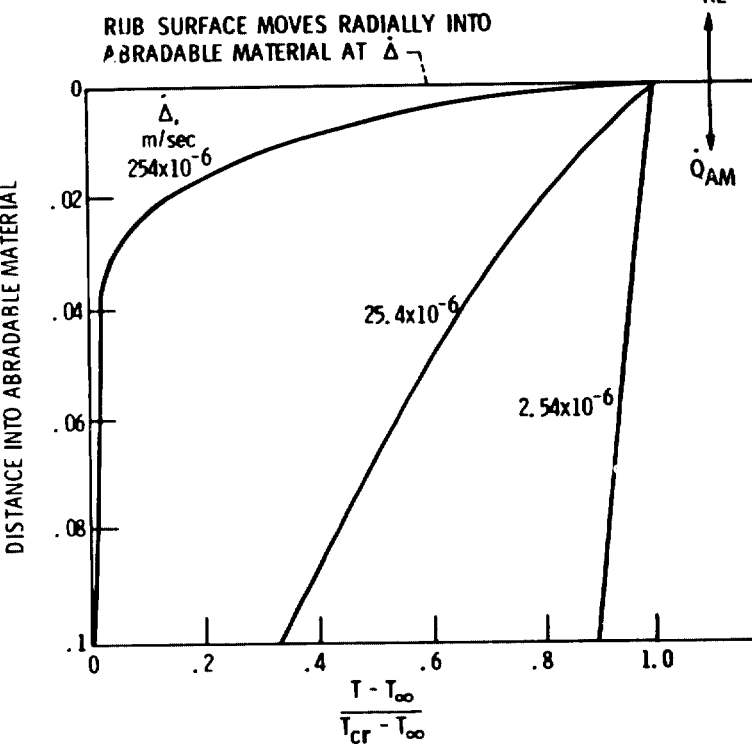


Figure 11. - Schematic representation of temperature profile beneath the sub surface, in the abradable material.



Figure 12. - Microsection through the rub groove on plasma-sprayed NiCr-glass coated fibermetal. Arrows indicate the glassy phase, and "F" denotes a region of densified fibermetal. Rotational speed was 183 m/sec, and the incursion rate was 254×10^{-6} m/sec.